Ultrabroadband terahertz spectroscopy of a liquid crystal

Vieweg, N.; Fischer, B. M.; Reuter, M.; Kula, P.; Dabrowski, R.; Celik, M. A.; Frenking, G.; Koch, M.; Jepsen, Peter Uhd

Published in:
Optics Express

Link to article, DOI:
10.1364/OE.20.028249

Publication date:
2012

Document Version
Publisher's PDF, also known as Version of record

Ultrabroadband terahertz spectroscopy of a liquid crystal

N. Vieweg,[1,3] B. M. Fischer,[1,2] M. Reuter,[1] P. Kula,[4] R. Dabrowski,[4] M. A. Celik,[5] G. Frenking,[5] M. Koch,[1] and P. U. Jepsen,[3]

[1] *Fachbereich Physik, Philipps-Universität Marburg, Hans-Meerwein-Straße MZG C06, 35032 Marburg, Germany*
[2] *Institut Franco-Allemand de recherches de Saint-Louis, 5 rue du Général Cassagnou, 68301 Saint-Louis Cedex, France*
[3] *Department of Photonics Engineering, Technical University of Denmark, Ørsteds Plads, 2800 Kgs. Lyngby, Denmark*
[4] *Institute of Chemistry, Military University of Technology, 00-908 Warsaw, Poland*
[5] *Faculty of Chemistry and Materials Sciences Center, Philipps-Universität Marburg, D-35032 Marburg, Germany*

Abstract: Liquid crystals (LCs) are becoming increasingly important for applications in the terahertz frequency range. A detailed understanding of the spectroscopic parameters of these materials over a broad frequency range is crucial in order to design customized LC mixtures for improved performance. We present the frequency dependent index of refraction and the absorption coefficients of the nematic liquid crystal 5CB over a frequency range from 0.3 THz to 15 THz using a dispersion-free THz time-domain spectrometer system based on two-color plasma generation and air biased coherent detection (ABCD). We show that the spectra are dominated by multiple strong spectral features mainly at frequencies above 4 THz, originating from intramolecular vibrational modes of the weakly LC molecules.

OCIS codes: (160.3710) Liquid crystals; (300.6495) Spectroscopy, terahertz.

References and links

1. T. S. Perova, "Far-infrared and low - frequency Raman spectra of condensed matter," Adv. Chem. Phys. **87**, 427–482 (1994).
2. G. J. Evans and M. W. Evans, "Far-infrared spectroscopy of liquid crystals," Infrared Phys. **18**(5-6), 863–866 (1978).
3. G. J. Evans, K. Moscicki, and M. W. Evans, "The Poley absorption in liquid crystals," J. Mol. Liq. **32**(2), 149–160 (1986).
4. F. Rutz, T. Hasek, M. Koch, H. Richter, and U. Ewert, "Terahertz birefringence of liquid crystal polymers," Appl. Phys. Lett. **89**(22), 221911 (2006).
5. N. Vieweg, M. K. Shakfa, B. Scherger, M. Mikulics, and M. Koch, "THz properties of nematic liquid crystals," J. Infrared Milli. Terahz. Waves **31**(11), 1312–1320 (2010).
6. N. Vieweg and M. Koch, "Terahertz properties of liquid crystals with negative dielectric anisotropy," Appl. Opt. **49**(30), 5764–5767 (2010).
7. M. Heng, S. De-Heng, H. Jun, and P. Yu-Feng, "Simulation study on terahertz vibrational absorption in liquid crystal compounds," Chin. Phys. B **18**(3), 1085–1088 (2009).
8. R. P. Pan, C. F. Hsieh, C. L. Pan, and C. Y. Chen, "Temperature-dependent optical constants and birefringence of nematic liquid crystal 5CB in the terahertz frequency range," J. Appl. Phys. **103**(9), 093523 (2008).
9. C. S. Yang, C. J. Lin, R. P. Pan, C. T. Que, K. Yamamoto, M. Tani, and C. L. Pan, "The complex refractive indices of the liquid crystal mixture E7 in the terahertz frequency range," J. Opt. Soc. Am. B **27**(9), 1866–1873 (2010).
10. H. Park, E. P. Parrott, F. Fan, M. Lim, H. Han, V. G. Chigrinov, and E. Pickwell-MacPherson, "Evaluating liquid crystal properties for use in terahertz devices," Opt. Express **20**(11), 11899–11905 (2012).
11. L. Beresnev and W. Haase, "Ferroelectric liquid crystals: development of materials and fast electrooptical elements for non-display applications," Opt. Mater. **9**(1-4), 201–211 (1998).
12. D. Engström, M. J. O'Callaghan, C. Walker, and M. A. Handschy, "Fast beam steering with a ferroelectric-liquid-crystal optical phased array," Appl. Opt. **48**(9), 1721–1726 (2009).
13. C. Y. Chen, C. F. Hsieh, Y. F. Lin, R. P. Pan, and C. L. Pan, "Magnetically tunable room-temperature 2 pi liquid crystal terahertz phase shifter," Opt. Express **12**(12), 2625–2630 (2004).

#177408 - $15.00 USD Received 3 Oct 2012; revised 23 Nov 2012; accepted 24 Nov 2012; published 5 Dec 2012

14. N. Vieweg, N. Born, I. Al-Naib, and M. Koch, "Electrically tunable terahertz notch filters," J Infrared Milli Terahz Waves **33**(3), 327–332 (2012).
15. T. Kleine-Ostmann and T. Nagatsuma, "A review on terahertz communications research," J Infrared Milli Terahz Waves **32**(2), 143–171 (2011).
16. J. Federici and L. Moeller, "Review of terahertz and subterahertz wireless communications," J. Appl. Phys. **107**(11), 111101 (2010).
17. U. M. S. Murthy and J. K. Vij, "Submillimetre wave spectroscopy of 4-n-alkyl-4′-cyano biphenyl liquid crystals," Liquid Cryst. **4**(5), 529–542 (1989).
18. P. U. Jepsen, D. G. Cooke, and M. Koch, "Terahertz spectroscopy and imaging – Modern techniques and applications," Laser Photon. Rev. **5,** 124–166 (2011); ibid. **6,** 418 (2012).
19. N. Vieweg, C. Jansen, M. K. Shakfa, M. Scheller, N. Krumbholz, R. Wilk, M. Mikulics, and M. Koch, "Molecular properties of liquid crystals in the terahertz frequency range," Opt. Express **18**(6), 6097–6107 (2010).
20. R. P. Pan, T. R. Tsai, C. Y. Chen, and C. L. Pan, "Optical constants of two typical liquid crystals 5CB and PCH5 in the THz frequency range," J. Biol. Phys. **29**(2/3), 335–338 (2003).
21. R. J. Falconer, H. A. Zakaria, Y. Y. Fan, A. P. Bradley, and A. P. J. Middelberg, "Far-infrared spectroscopy of protein higher-order structures," Appl. Spectrosc. **64**(11), 1259–1264 (2010).
22. J. M. Dai, X. F. Lu, J. Liu, I. C. Ho, N. Karpowicz, and X C. Zhang, "Remote THz wave sensing in ambient atmosphere," Science **2**, 131–143 (2009).
23. D. G. Cooke, F. C. Krebs, and P. U. Jepsen, "Direct observation of sub-100 fs mobile charge generation in a polymer-fullerene film," Phys. Rev. Lett. **108**(5), 056603 (2012).
24. J. Dai, J. Liu, and X. C. Zhang, "Terahertz wave air photonics: Terahertz wave generation and detection with laser-induced gas plasma," IEEE J. Sel. Top. Quantum Electron. **17**(1), 183–190 (2011).
25. D. J. Cook and R. M. Hochstrasser, "Intense terahertz pulses by four-wave rectification in air," Opt. Lett. **25**(16), 1210–1212 (2000).
26. M. Kress, T. Löffler, S. Eden, M. Thomson, and H. G. Roskos, "Terahertz-pulse generation by photoionization of air with laser pulses composed of both fundamental and second-harmonic waves," Opt. Lett. **29**(10), 1120–1122 (2004).
27. X. Xie, J. Dai, and X. C. Zhang, "Coherent control of THz wave generation in ambient air," Phys. Rev. Lett. **96**(7), 075005 (2006).
28. J. Dai, X. Xie, and X. C. Zhang, "Detection of Broadband Terahertz Waves with a Laser-Induced Plasma in Gases," Phys. Rev. Lett. **97**(10), 103903 (2006).
29. M. Zalkovskij, C. Z. Bisgaard, A. Novitsky, R. Malureanu, D. Savastru, A. Popescu, P. U. Jepsen, and A. V. Lavrinenko, "Ultrabroadband terahertz spectroscopy of chalcogenide glasses," Appl. Phys. Lett. **100**(3), 031901 (2012).
30. S. N. Taraskin, S. I. Simdyankin, S. R. Elliott, J. R. Neilson, and T. Lo, "Universal features of terahertz absorption in disordered materials," Phys. Rev. Lett. **97**(5), 055504 (2006).
31. A. F. Ioffe and A. R. Regel, "Non-crystalline, amorphous, and liquid electronic semiconductors," Prog. Semicond. **4**, 237–291 (1960).
32. M. E. Mullen, B. Lüthi, and M. J. Stephen, "Sound velocity in a nematic liquid crystal," Phys. Rev. Lett. **28**(13), 799–801 (1972).
33. P. U. Jepsen and S. J. Clark, "Precise ab-initio prediction of terahertz vibrational modes in crystalline systems," Chem. Phys. Lett. **442**(4-6), 275–280 (2007).
34. M. J. Frisch, G. W. Trucks, H. B. Schlegel, G. E. Scuseria, M. A. Robb, J. R. Cheeseman, G. Scalmani, V. Barone, B. Mennucci, G. A. Petersson, H. Nakatsuji, M. Caricato, X. Li, H. P. Hratchian, A. F. Izmaylov, J. Bloino, G. Zheng, J. L. Sonnenberg, M. Hada, M. Ehara, K. Toyota, R. Fukuda, J. Hasegawa, M. Ishida, T. Nakajima, Y. Honda, O. Kitao, H. Nakai, T. Vreven, J. J. A. Montgomery, J. E. Peralta, F. Ogliaro, M. Bearpark, J. J. Heyd, E. Brothers, K. N. Kudin, V. N. Staroverov, R. Kobayashi, J. Normand, K. Raghavachari, A. Rendell, J. C. Burant, S. S. Iyengar, J. Tomasi, M. Cossi, N. Rega, N. J. Millam, M. Klene, J. E. Knox, J. B. Cross, V. Bakken, C. Adamo, J. Jaramillo, R. Gomperts, R. E. Stratmann, O. Yazyev, A. J. Austin, R. Cammi, C. Pomelli, J. W. Ochterski, R. L. Martin, K. Morokuma, V. G. Zakrzewski, G. A. Voth, P. Salvador, J. J. Dannenberg, S. Dapprich, A. D. Daniels, Ö. Farkas, J. B. Foresman, J. V. Ortiz, J. Cioslowski, and D. J. Fox, "Gaussian 09," (2009).
35. A. D. Becke, "Density-functional exchange-energy approximation with correct asymptotic behavior," Phys. Rev. A **38**(6), 3098–3100 (1988).
36. J. P. Perdew, "Density-functional approximation for the correlation energy of the inhomogeneous electron gas," Phys. Rev. B 33, 8822–8824, Erratum: B **34**, 7406 (1986).
37. A. Schäfer, H. Horn, and R. Ahlrichs, "Fully optimized contracted Gaussian basis sets for atoms Li to Kr," J. Chem. Phys. **97**(4), 2571–2575 (1992).
38. T. Hanemann, W. Haase, I. Svoboda, and H. Fuess, "Crystal structure of the 4'-pentyl-4-cyanobiphenyl (5CB)," Liquid Cryst. **19**(5), 699–702 (1995).

1. Introduction

A relatively new but remarkably fast growing research topic is the investigation and characterization of the terahertz (THz) spectral properties of liquid crystals (LCs) [1–10].

#177408 - $15.00 USD Received 3 Oct 2012; revised 23 Nov 2012; accepted 24 Nov 2012; published 5 Dec 2012

These studies are spurred by an increased demand for new fast and cost-efficient switchable devices [11], to manipulate the THz radiation for various applications [12–14] including THz communication [15,16]. As the properties of LCs are typically optimized for applications in the visible part of the electromagnetic spectrum, a customized design of new LC mixtures targeted for applications in the THz range, however, requires detailed knowledge of the dielectric properties over a broad frequency range. Among the most comprehensively investigated LC materials in this frequency range are 4'-pentyl-4-cyanobiphenyl (5CB) and other members of the CB family. These relatively simple structured LCs are found in many recent LC mixtures. Therefore, an extensive database exists for these molecules for the optical, near- and mid-IR frequency range down to approximately 400 cm^{-1}, i.e. approximately 12 THz. In contrast, only very few reports based on Fourier transform infrared (FTIR) spectroscopy data accessing the far-infrared or THz frequency range below 10 THz, exist [17]. The sparse published data indicate that the spectra of most members of the CB family molecules are richly structured by various strong resonances. Polarization-dependent spectra have until now not been obtained with this measurement scheme, and in particular the lower frequency part suffers from a considerable uncertainty.

THz time domain-spectroscopy (THz-TDS) offers a versatile alternative to FTIR for the recording of the polarization dependent absorption as well as index of refraction in the terahertz frequency range [18]. Therefore, significantly more data has become available recently, reporting these parameters for various members of the CB family [19,20]. However, these data are typically limited to frequencies below approximately 2.5 THz. At these low frequencies, nearly no spectroscopic features are observed. In some few cases, the rising slope of a strong feature at higher frequencies can be observed. The most interesting, richly structured frequency band, containing the lowest vibrational modes of the systems and thus bridging the featureless low frequency THz data and the IR data, still remains unexplored.

Recently, a new emission and detection scheme based on photo mixing in air plasma has been demonstrated and applied for ultrabroadband spectroscopy. This new technology already has had a significant impact on THz applications, as it combines a broadband detection scheme with remote sensing technology. As the spectra of many materials such as proteins [21], explosives [22], but also liquid crystals typically exhibit the most pronounced characteristic signatures in the frequency range above 2 THz, this technique enables to really fully exploit the detection and identification potential of THz technologies.

Here we present the refractive indices n_e and n_o for extraordinary and ordinary polarization, respectively; as well as the absorption coefficients for both polarizations over the extended frequency range between approximately 200 GHz to 15 THz. The data was recorded using an air biased coherent detection (ABCD) system. We compare our data with previous work in the lower THz frequency range. Several very strong, specific signatures, which vary mainly in their intensity with respect to the polarization, are observed.

2. Liquid crystal material

The liquid crystal investigated here is 4'-pentyl-4-cyanobiphenyl (5CB). In contrast to many other commercial LCs, the structure of 5CB is simple and well known, making it an ideal candidate for scientific studies. It consists of a biphenyl core, a cyano group (CN) on one side and an alkyl chain (C_5H_{11}) on the other side. The structure of 5CB is shown in Fig. 1. The molecule is liquid crystalline at room temperature.

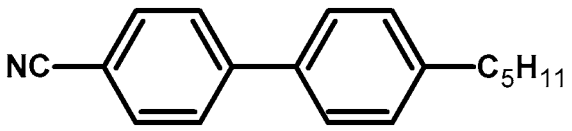

Fig. 1. Molecular structure of 4'pentyl-4-cyanobiphenyl (5CB).

#177408 - $15.00 USD Received 3 Oct 2012; revised 23 Nov 2012; accepted 24 Nov 2012; published 5 Dec 2012

3. Experimental procedure

The spectra are recorded using a spectroscopy system based on two-color laser plasma THz generation and air biased coherent detection (ABCD) [23]. A schematic of the system is shown in Fig. 2, and a general description of the air plasma based generation and detection can be found in [24]. Specifically, THz transients are generated by focusing a beam of 1mJ, 35-fs pulses at 800 nm center wavelength and f_{rep} = 1 kHz repetition frequency together with the second harmonic of the beam, generated collinearly with the fundamental in a 100 μm thick β-BBO crystal, to form a plasma. A half wave plate for 400 nm rotates the polarization of the 400 nm light to match that of the 800 nm fundamental. A combination of four wave mixing due to the third-order nonlinearity of the air and nonlinear currents in the plasma driven by the laser field [25,26] generates ultrabroadband THz transients, limited in duration and bandwidth only by the duration of the pump laser pulses. The generation efficiency depends critically on the phase difference between the fundamental and second harmonic of the pump beam [27]. We optimize the phase difference by adjusting the distance between the BBO crystal and the focal region.

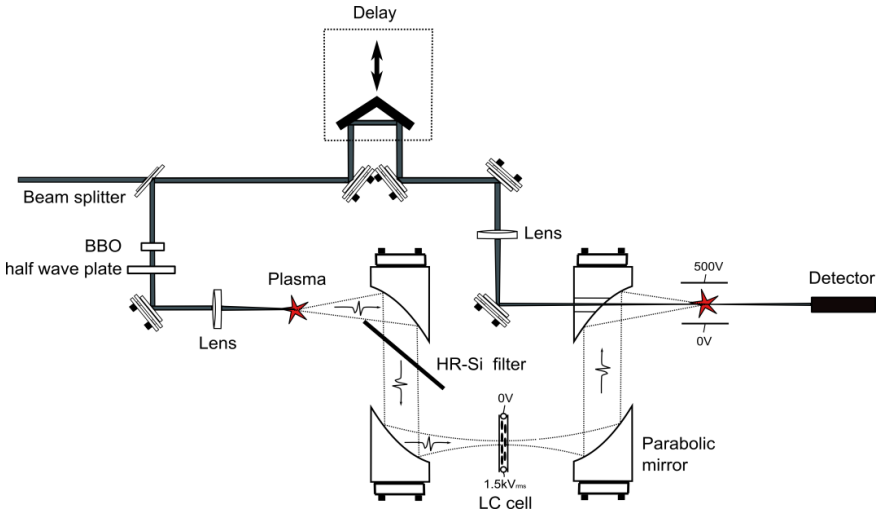

Fig. 2. Schematic of the experimental setup.

The generated THz beam is collimated and refocused by a pair of off-axis paraboloidal mirrors to an intermediate focal plane, where the sample is placed. After the intermediate focus, two additional off-axis paraboloidal mirrors recollimate, guide and focus the beam to the ABCD unit. ABCD, as described elsewhere [28], is used for detection of the temporal profile of the THz transient, by slow scanning of a delay stage in the 800-nm wavelength probe beam path while recording the intensity of THz-induced second harmonic generation in the detection region with a photomultiplier tube. An applied DC voltage across the detection region serves as optical bias, thereby enabling field-resolved detection of the THz transient.

Figure 3 represents (a) a typical reference pulse and (b) its corresponding amplitude spectrum (b). The highest accessible frequency of the system is approximately 40 THz and it has a signal-to-noise ratio of 55dB at 5THz. The THz pulses are polarized linearly. There has been one polarizer employed before the cell, but none after the cell. As the detector is polarization sensitive, it itself acts as a polarizer.

#177408 - $15.00 USD Received 3 Oct 2012; revised 23 Nov 2012; accepted 24 Nov 2012; published 5 Dec 2012

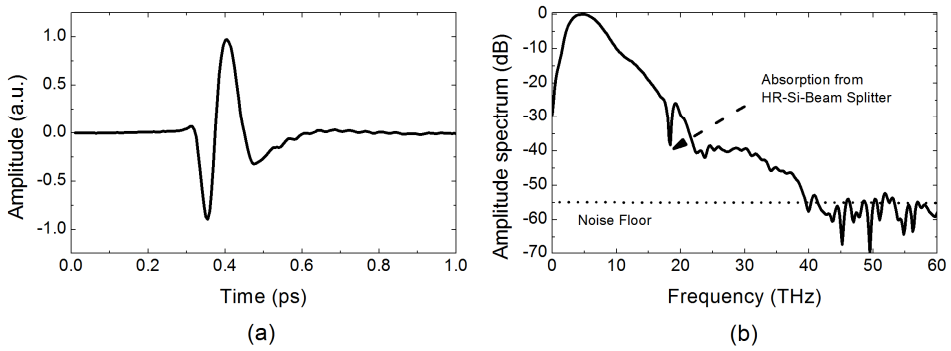

Fig. 3. (a) Measured time trace of the THz transient and (b) its corresponding spectrum.

The nematic liquid crystals are filled in a specifically designed cell consisting of two 2 mm thick TOPAS windows (Fig. 4). Metal wires between the windows act as both electrodes and spacers to cell thickness of d = 500 μm. The lateral distance between the wires, i.e., the width of the cell is 30 mm. A peak voltage of 1.5 kV at a modulation frequency of 1 kHz is applied to align the LCs. The cell can be rotated by 90° in order to perform measurements with the LCs aligned parallel or orthogonal to the polarization of the THz beam. The cell is kept at ambient temperature 22°C and no active temperature stabilization is applied.

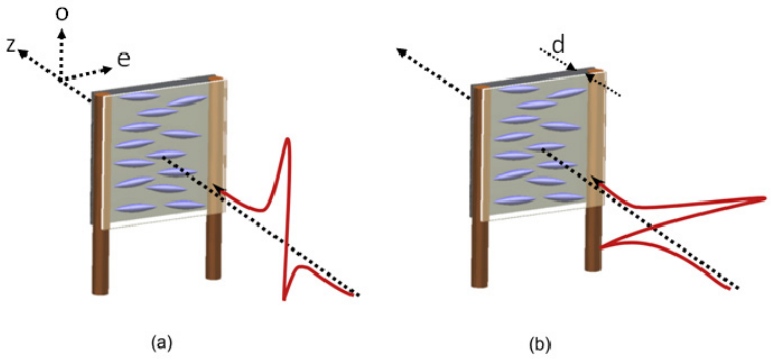

Fig. 4. THz pulse polarized (a) perpendicular (ordinary, o) and (b) parallel (extraordinary, e) to the preferred direction of the LC molecules

4. Experimental results

The 5CB was prepared at MUT Warsaw and stored under dry nitrogen atmosphere. It has the following phase transitions: Cr 23 N 37.2 Iso, purity >99.95% tested by GC-FID. Figure 5(a) shows the temporal trace of a reference pulse propagating through the empty sample cell compared to the pulses propagating through the loaded cell with the LCs aligned parallel to the polarization of the THz beam and rotated by 90°, respectively. The corresponding amplitude spectrum of the three pulses is shown in Fig. 5(b), together with the reference spectrum, recorded after transmission through the empty cell. The strong absorption band seen in the reference spectrum near 15 THz is due to absorption in the TOPAS polymer. Pronounced spectroscopic features are observed over the entire frequency range, in particular between 4 to 6 THz and above approximately 11 THz. The frequency-dependent absorption coefficient $\alpha(\nu)$ and index of refraction $n(\nu)$ are calculated from the complex ratio of the spectra of the THz transient transmitted through a filled cell and an empty cell, respectively.

#177408 - $15.00 USD Received 3 Oct 2012; revised 23 Nov 2012; accepted 24 Nov 2012; published 5 Dec 2012

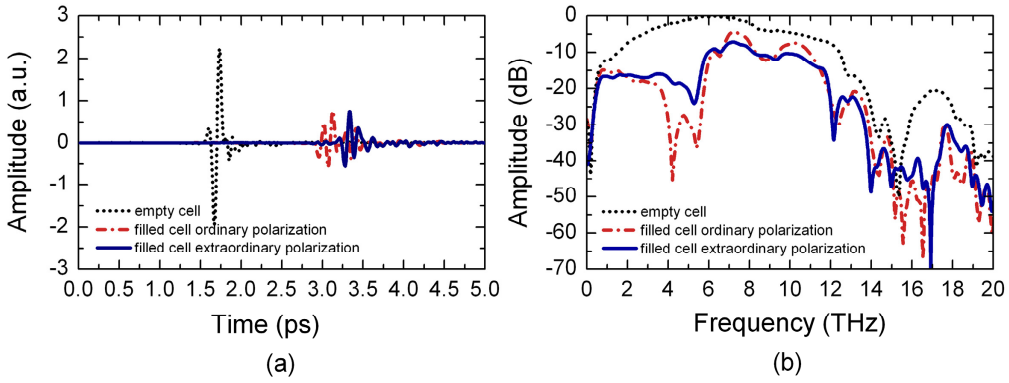

Fig. 5. (a) Reference pulse (empty cell) and sample pulses for ordinary and extraordinary polarization and (b) corresponding amplitude spectra.

The frequency dependent refractive indices n_o and n_e for ordinary and extraordinary polarization are shown in Fig. 6(a). For comparison, the data of an earlier measurement using a time-domain spectrometer with lower bandwidth [19] is also shown. This earlier work in the lower THz frequency range suggested an increasing birefringence with increasing frequency. Our data clearly shows that the average birefringence remains relatively constant at approximately $\Delta n \approx 0.14$ above 2 THz and over the entire frequency range up to 15 THz, with local variations in the vicinity of a resonance. For the low frequencies, an almost perfect overlap of the data acquired by the two different systems based on completely different technologies is observed.

Figure 6(b) shows the absorption coefficient α_o and α_e of 5CB for ordinary and extraordinary polarization, respectively, together with the previously obtained THz-TDS data for low frequencies. Again, a very good agreement between the latter and the new ABCD data is observed. A monotonous increase in the absorption coefficient is observed at low frequencies. Strong spectroscopic features dominate the spectra in particular between 4 and 6 THz and above 11 THz, with an area of relatively low absorption and small dichroism in between. Interestingly, a similar general behavior was observed in soft glasses [29] where the low-frequency region is dominated by a universal absorption observed in disordered materials [30] while localized, ordered vibrational modes appear above a characteristic frequency known as the Ioffe-Regel transition frequency [31]. This crossover behavior indicates that vibrational modes observed at higher frequencies are localized to small volumes within the sample. As an indicative estimate, we observe an approximate cross-over frequency between universal absorption and discrete absorption lines of 1 THz. Using a sound velocity of 1500 m/s (1.5 nm/ps) [32], the Ioffe-Regel crossover acoustic wavelength is 1.5 nm, indicating that vibrational order will be present only at length scales comparable or shorter than that. In a disordered system the linear absorption coefficient $\alpha(\omega)$ can be described as the product of the vibrational density of states $g(\omega)$ and the coupling coefficient between the electromagnetic wave and the vibrations $C(\omega)$, so that $\alpha(\omega) = C(\omega)g(\omega)$. For uncorrelated charge fluctuations, as have been observed in glassy systems in the low THz range [30] $C(\omega)$ is constant with frequency. We observe a linear frequency dependence of the absorption coefficient at low frequencies, indicating that the density of states is proportional to frequency. Thus, we can interpret the absorption spectrum as an indicator of a largely localized vibrational response of the individual molecules of the liquid crystal, in contrast to a global, phonon-like behavior observed in molecular crystals with a high degree of order [33].

The intensities of the absorption features are strongly dependent on the respective polarization, which gives already a first indication on the orientation of the dipole moment of the corresponding molecular vibration. For example, the features at approximately 12 and 14 THz are of comparable intensity, whereas the intensity of the feature at approximately 4.5

#177408 - $15.00 USD Received 3 Oct 2012; revised 23 Nov 2012; accepted 24 Nov 2012; published 5 Dec 2012

THz is significantly more pronounced in the absorption spectrum with the cells aligned in ordinary polarization geometry. It is expected that anticipated extended studies on different derivatives of the CB family, where individual atoms or small molecular groups are selectively exchanged, will provide further insight in the origin of these feature and thus the molecular vibrations.

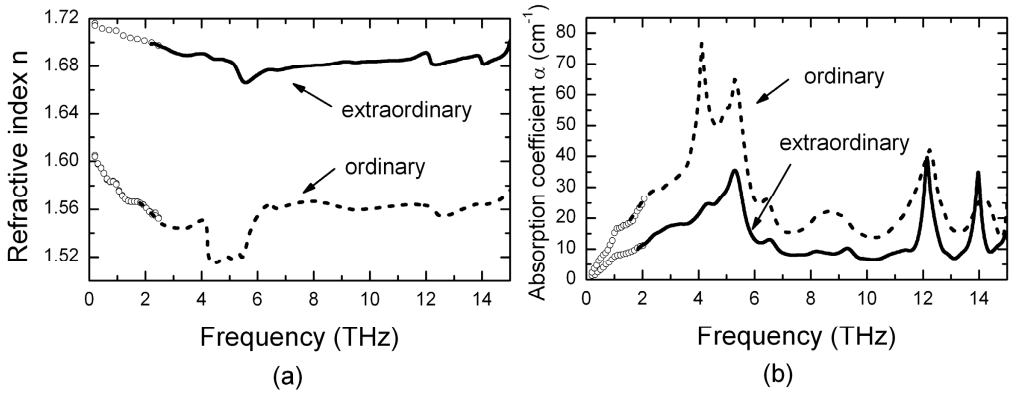

Fig. 6. (a) Extraordinary and ordinary index of refraction n_e and n_o, and (b) polarization dependent absorption coefficient of 5CB. For comparison, the results obtained previously with a conventional THz TDS system below 2 THz are shown (open circles).

When heated, the LC material approaches the phase transition temperature (nematic/isotropic) and gradually loses its anisotropic properties. Thus, e.g. the two absorption curves for extraordinary and ordinary polarization approach each other and overlap in the isotropic phase. We would expect a significant redshift and broadening of the resonances with increasing temperature, as a direct result of the increased thermally induced disorder and softening of anharmonic vibrational ladders.

5. Calculations

In order to deduce some information on the origin of the observed absorption features, we have calculated the absorption spectra of a 5CB molecule using density functional theory. The calculations were performed using the Gaussian 09 electronic structure program [34]. Both the geometry optimization and the frequency calculations of 5CB were carried out using BVP86 functional [35,36] with def2-SVP basis set [37]. The calculation is based on a single molecule at 0 K. Thus, the calculation offers no information about intermolecular interactions, including the influence of disorder. However, this isolated-molecule approach to the calculation of the vibrational spectrum of the liquid crystal is justified by our experimental indication of localization of the vibrational modes to individual molecules as well as by the lack of strong intermolecular hydrogen bonds in the LC matrix [38]. For simplicity, the polarization dependence has not been considered here. Therefore, while the calculations give some insight in the origin of the molecular vibrations that can be expected in this frequency range, they are not used as a reference for assigning the individual modes observed in the experimental spectrum.

The calculated vibrational frequencies and their intensities (blue bars) are shown in Fig. 7. The discrete frequency values are broadened using Gaussian profiles, in order to facilitate a comparison with the experimental data. The widths are set to mimic the experimentally observed line widths. Similarly to the experimental spectrum, strong bands below 6 THz and a second set of stronger bands above 12 THz are observed. Although a direct assignment is not possible with this preliminary theoretical data, it is worth to note that even at low frequencies prominent intramolecular vibrations occur. Below 3 THz we determine a discrepancy between the observed and calculated spectra. We attribute the difference to the

#177408 - $15.00 USD Received 3 Oct 2012; revised 23 Nov 2012; accepted 24 Nov 2012; published 5 Dec 2012

disorder-induced coupling between the electromagnetic field and the vibrational density of states at low frequencies, which is not considered in the calculation. A further refinement of the calculations is thus expected to allow for a direct assignment of at least some of the experimentally observed modes.

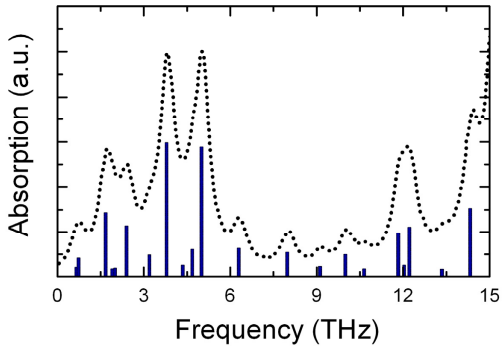

Fig. 7. Calculated absorption spectrum of 5CB (not polarization dependent). The dotted line represents a Gaussian fit.

6. Conclusion

We have shown that by using a dispersion-free, air photonics-based THz-TDS system, the polarization dependent spectra of 5CB between approximately 300 GHz and 12 THz can be recorded. At low frequencies (< 2 THz) we see strong indications of disorder-induced, universal absorption, indicating that the vibrational response is largely due to individual, molecular vibrational modes, and we observe several strong resonance features over the entire frequency range above approximately 2.5 THz, i.e. above the frequency band which has previously been accessed with conventional THz time-domain spectroscopy. The potential of ultrabroadband THz-TDS to bridge the spectroscopic gap between the THz and IR frequency bands is thus further emphasized. The results are expected to increase the knowledge on the low-frequency vibrations giving rise to the observed spectral signatures. A detailed understanding of the THz dielectric properties of these materials is expected to allow for optimizing the custom designed LC mixtures for applications in modulation devices for THz radiation.

Acknowledgments

We thank Dr. David G. Cooke (McGill University) for assistance with air photonics. Nico Vieweg thanks the German Academic Exchange service (DAAD) for funding. The Carlsberg Foundation and H. C. Ørsteds Foundation are acknowledged for partial financial support.

#177408 - $15.00 USD Received 3 Oct 2012; revised 23 Nov 2012; accepted 24 Nov 2012; published 5 Dec 2012